Sub-Gridding FDTD Schemes

PETER MONK
Department of Mathematical Sciences
University of Delaware, Newark, DE 19716
monk@math.udel.edu

Abstract

Local meshing or sub-gridding has been advocated by a number of authors as a way of increasing the spatial resolution of the finite difference time domain method (FDTD). In this paper we show how to use supraconvergence to analyze the error in a simple sub-gridding strategy in two dimensions. We also analyze the spurious reflection that occurs at an interface between two grids for the standard FDTD scheme, for simple subgridding method and for another subgridding scheme employing linear interpolation. The overall order of convergence of the reflection coefficients is the same for all the methods, but the linear scheme has a lower amplitude spurious transmitted mode compared to the simple subgridding scheme.

Keywords: Maxwell's equations, Yee's scheme, Sub-gridded meshes, error estimates.

1 Introduction

In this paper we shall describe the state of the art of the error analysis of Yee's finite difference time domain scheme (FDTD) [1]. Except on uniform grids of identical cubes (or squares in two dimensions), it is necessary to use "supraconvergence" techniques to obtain the correct order of convergence of the method [2, 3]. These techniques essentially involve a standard finite difference analysis of consistency and stability allowing for special interactions between the stability and consistency properties of the method.

Here we shall analyze the convergence of two modifications to the basic Yee scheme which attempt to handle sub-gridding [4, 5, 6, 7]. A sub-grided Yee scheme is one that uses multiple mesh sizes in a single simulation with an abrupt transition between regions of different sized elements. At the interface between meshes of different size, the classical Yee FDTD scheme has to be modified and this modification has to be done in a way that prevents excessive numerical reflection from the interface. We shall analyze two such methods, the first being a very simple method motivated by the work of Ewing et. al. [8]. In this method, piecewise constant interpolation is used to obtain field values required by the finite difference scheme. Remarkably, the resulting scheme seems to be second order accurate (by numerical experiments). Using a supraconvergence analysis, we will prove three halves order accuracy. We shall also provide a reflection analysis at the interface, supporting the observation of second order convergence. The second method we shall analyze is similar to the method proposed by Kim and Hoefer [5] in that piecewise linear interpolation is used in the development of the extended FDTD scheme. Using a reflection analysis, we shall show how this method improves on the simple scheme. Piecewise quadratic interpolation has been proposed in [6]. We shall not analyze that method here, but our analysis of the other two methods suggests that quadratic interpolation may not be necessary.

Sub-gridding schemes have been studied in other areas, for example in wave propagation [9]. A particularly important paper in the development of the method is [10] which deals with time-stepping issues. In this paper we shall only concentrate on spatial discretization. Time stepping is also obviously a very important aspect of the problem and we hope to incorporate this into the analysis at a later date.

2 The Model Problem

For simplicity we shall restrict our analysis to the Maxwell system in two space dimensions (TM mode). In this case the magnetic field is polarized parallel to the axis of an infinite cylindrical scatter. Hence the magnetic field can be represented by a scalar quantity. The electric field is a vector normal to the axis of the cylinder and hence has two components. We expect that our method of analysis will carry over to three dimensions.

The problem we shall approximate is the following. Let $\Omega = [-L, L]^2, L > 0$ be a square domain. As in our previous work, the extension of our estimates to more complex domains consisting of unions of squares is possible. We want to approximate the electric field $\boldsymbol{E}(\boldsymbol{x},t) = (E^{(1)}(\boldsymbol{x},t), E^{(2)}(\boldsymbol{x},t))^T$ and magnetic field $H(\boldsymbol{x},t)$ (here the superscript T denotes transpose, $\boldsymbol{x} = (x_1,x_2)^T$ is the spatial coordinate, and t is time) which satisfy the Maxwell System

$$\begin{aligned} \frac{\partial \boldsymbol{E}}{\partial t} - \vec{\nabla} \times H &= -\boldsymbol{J} \text{ in } \Omega, && \text{(1a)} \\ \frac{\partial H}{\partial t} + \nabla \times \boldsymbol{E} &= 0 \text{ in } \Omega. && \text{(1b)} \end{aligned}$$

Here $\boldsymbol{J}(\boldsymbol{x},t)$ is a given current density, and

$$\vec{\nabla} \times H = \begin{pmatrix} \dfrac{\partial H}{\partial y} \\ -\dfrac{\partial H}{\partial x} \end{pmatrix}, \quad \nabla \times \boldsymbol{E} = \frac{\partial}{\partial x} E^{(2)} - \frac{\partial}{\partial y} E^{(1)}.$$

The analysis of the error in the FDTD approximation of the extension of (1a)–(1b) that incorporates smoothly varying electromagnetic parameters ϵ and μ, and a smooth conductivity follows the same lines as the analysis given here. Step changes in these parameters would require a new analysis.

In addition to the differential equation, we shall assume a perfectly conducting boundary condition:

$$\boldsymbol{n} \times \boldsymbol{E} = 0 \text{ on } \partial\Omega \qquad (2)$$

where $\boldsymbol{n}$ is the unit outward normal to Ω and $\partial\Omega$ is the boundary of Ω. Finally, we assume given initial data

$$\boldsymbol{E}(\boldsymbol{x},0) = \boldsymbol{E}_0(\boldsymbol{x}) \text{ and } H(\boldsymbol{x},0) = H_0(\boldsymbol{x}) \text{ in } \Omega \qquad (3)$$

where $\boldsymbol{E}_0$ and H_0 are known functions.

3 Standard Yee Scheme

As a reference configuration, we first describe the standard Yee scheme on a step grid in which the grid cells are suddenly compressed in one direction. This is not yet a sub-grid since the step grid is refined in one direction only and still has the standard mesh structure. More precisely, for $x < 0$ we assume that a standard Yee grid has been used with a mesh having cells of size $2h$ where $h > 0$. For $x > 0$ the cells are of length h in the x direction and of length $2h$ in the y direction. Thus at $x = 0$ the cells are suddenly compressed in the x direction. Figure 1 shows a typical grid. Obviously this type of grid would only be used if there were features in the region $x > 0$ that could be better resolved using a compressed grid.

We define the grid parameter $h = L/(2N)$, $N > 0$ where N is an integer. The horizontal grid lines are at $y = y_{2l} = 2lh$, $-N \le l \le N$. For $x \le 0$ the vertical grid lines are at $x = x_{2l} = 2lh$, $-N \le l \le 0$ and for $x > 0$ they are at $x = x_l = lh$, $0 \le l \le 2N$. In the Yee FDTD scheme, the electric field variables are associated with edges of the grid. Thus the finite difference electric field unknowns are (taking into account the zero boundary data):

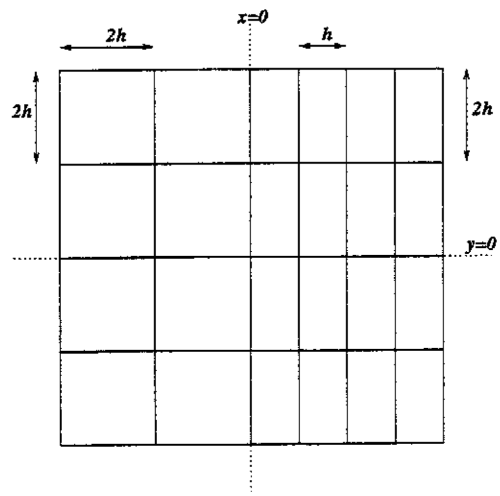

Figure 1: A typical grid for the standard Yee scheme analyzed in this paper. A compressed grid and a uniform grid meet at $x = 0$.

$$E^{(1)}_{p,q} \simeq E^{(1)}(x_p, y_q, t)$$

for $q = 2l$, $-N+1 \le l \le N-1$ and

$$p = \begin{cases} 2r+1 & \text{if } -N \le r < 0, \\ p = r + \frac{1}{2} & \text{if } 0 < r < 2N; \end{cases}$$

and

$$E^{(2)}_{p,q} \simeq E^{(2)}(x_p, y_q, t)$$

for $q = 2l+1$, $-N \le l < N$ and

$$p = \begin{cases} 2r & \text{if } -N+1 \le r \le 0, \\ r & \text{if } 0 \le r < 2N. \end{cases}$$

Magnetic FDTD variables are associated with the centroid of the grid cells so

$$H_{p,q} \simeq H(x_p, y_q, t) \begin{cases} q = 2l+1 & -N \le l < N, \\ p = 2r+1 & -N \le r < 0, \\ p = r + \frac{1}{2} & 0 \le r < 2N. \end{cases}$$

The standard Yee FDTD scheme [1] is used for all variables associated with points with $x < 0$ (i.e., in the uniform grid). Similarly, the contour path extension of the Yee scheme (see for example [11]) is used to discretize the problem for $x \ge 0$. Figure 2 shows cells either side of $x = 0$ and shows the location of the degrees of freedom. Since the equations for Yee's scheme are well-known we

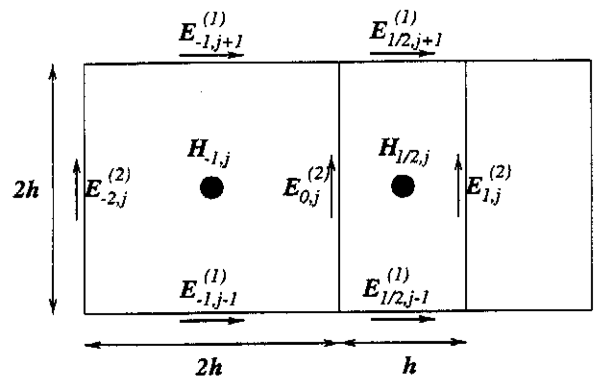

Figure 2: A diagram of the cells either side of $x = 0$. Here $j = 2l + 1$ for some l with $-N \le l < N$. At $x = 0$ the grid size changes abruptly.

will only write down those for the two cells adjoining $x = 0$ in Figure 2.

$$4h^2\frac{dE^{(1)}_{-1,j+1}}{dt} - 2h\left(H_{-1,j+2} - H_{-1,j}\right) \qquad \text{(4a)}$$
$$= -4h^2 J^{(1)}_{-1,j+1},$$
$$4h^2\frac{dE^{(2)}_{-2,j}}{dt} - 2h(H_{-3,j} - H_{-1,j}) \qquad \text{(4b)}$$
$$= -4h^2 J^{(2)}_{-2,j},$$
$$4h^2\frac{dH_{-1,j}}{dt} + 2h\Big[(E^{(2)}_{0,j} - E^{(2)}_{-2,j}) \qquad \text{(4c)}$$
$$-(E^{(1)}_{-1,j+1} - E^{(1)}_{-1,j-1})\Big] = 0,$$
$$3h^2\frac{dE^{(2)}_{0,j}}{dt} - 2h(H_{-1,j} - H_{1/2,j}) = -3h^2 J^{(2)}_{0,j}, \text{(4d)}$$
$$2h^2\frac{dE^{(1)}_{1/2,j+1}}{dt} - h\left(H_{1/2,j+2} - H_{1/2,j}\right) \qquad \text{(4e)}$$
$$= -2h^2 J^{(1)}_{1/2,j+1},$$
$$2h^2\frac{dE^{(2)}_{1,j}}{dt} - 2h(H_{1/2,j} - H_{3/2,j}) = -2h^2 J^{(2)}_{1,j}, \text{(4f)}$$
$$2h^2\frac{dH_{1/2,j}}{dt} + 2h(E^{(2)}_{1,j} - E^{(2)}_{0,j}) \qquad \text{(4g)}$$
$$-h(E^{(1)}_{1/2,j+1} - E^{(1)}_{1/2,j-1}) = 0,$$

where $j = 2l + 1$ and $-N \le l < N$. Here $J^{(\gamma)}_{\alpha,\beta} = J^{(\gamma)}(x_\alpha, y_\beta, t)$. By numbering the electric field unknowns and the magnetic field unknowns we can form two vectors $\vec{E}$ and $\vec{H}$ of the unknown field values. Then if we number the discrete currents in the same way as the electric field, we can write the finite difference equations in matrix form:

$$M_E\frac{d}{dt}\vec{E} - C\vec{H} = -M_E\vec{J}, \qquad \text{(5a)}$$

$$M_H\frac{d}{dt}\vec{H} + C^T\vec{E} = 0. \qquad \text{(5b)}$$

The matrices M_E and M_H are diagonal with diagonal entries either $4h^2$ (if the corresponding unknown is in $x < 0$), $2h^2$ (if the unknown is in $x > 0$) or $3h^2$ (if the unknown is on $x = 0$). Of key importance to the stability of the scheme is that the curl matrix for the electric and magnetic fields are related by transposition. In [2] we proved stability for a generalization of (5a)–(5b), however this generalization is insufficient to handle the sub-gridding algorithms analyzed in this paper. So we next prove a stability result for a generalization of (5a)–(5b). To do this we define two mesh dependent discrete norms for the discrete electric and magnetic fields respectively:

$$|||\vec{E}|||_E = \sqrt{(\vec{E})^T M_E \vec{E}},$$
$$|||\vec{H}|||_H = \sqrt{(\vec{H})^T M_H \vec{H}}.$$

Theorem 3.1 *Suppose $\vec{E}$ and $\vec{H}$ satisfy the system of differential equations:*

$$M_E\frac{d}{dt}\vec{E} - C\vec{H} = C\vec{\beta} + M_E\vec{\gamma} \qquad \text{(6a)}$$
$$M_H\frac{d}{dt}\vec{H} + C^T\vec{E} = C^T\vec{\delta} + M_H\vec{\alpha} \qquad \text{(6b)}$$

where $\vec{\alpha}$, $\vec{\beta}$, $\vec{\delta}$ and $\vec{\gamma}$ are given continuous vector functions of time. In addition suppose at $t = 0$, $\vec{H} = 0$, $\vec{E} = 0$. Then there exists a constant c independent of t such that

$$|||\vec{E}(t)|||_E + |||\vec{H}(t)|||_H \le c\left(\max_{0\le s\le t}|||\vec{\beta}(s)|||_H + \max_{0\le s\le t}|||\vec{\delta}(s)|||_E + \int_0^t \left(|||\vec{\alpha}(s)|||_H + |||\vec{\gamma}(s)|||_E + |||\frac{d\vec{\beta}}{dt}(s)|||_H + |||\frac{d\vec{\delta}}{dt}(s)|||_E\right) ds.\right).$$

Proof. Rewriting (6a) and (6b) we have

$$M_E\frac{d}{dt}\left(\vec{E} - \vec{\delta}\right) - C\left(\vec{H} + \vec{\beta}\right) = M_E\left(\vec{\gamma} - \frac{d}{dt}\vec{\delta}\right),$$
$$M_H\frac{d}{dt}\left(\vec{H} + \vec{\beta}\right) + C^T\left(\vec{E} - \delta\right) = M_H\left(\vec{\alpha} + \frac{d}{dt}\vec{\beta}\right).$$

Multiplying the first equation by $\left(\vec{E} - \vec{\delta}\right)^T$ and the second by $\left(\vec{H} + \vec{\beta}\right)^T$ and adding we obtain (since the curl terms cancel)

$$\frac{1}{2}\frac{d}{dt}\left(|||\vec{E}-\vec{\delta}|||_E^2+|||\vec{H}+\vec{\beta}|||_H^2\right)$$
$$\leq |||\vec{E}-\vec{\delta}|||_E\,|||\vec{\gamma}-\frac{d}{dt}\vec{\delta}|||_E$$
$$+|||\vec{H}+\vec{\beta}|||_H\,|||\vec{\alpha}+\frac{d}{dt}\vec{\beta}|||_H.$$

Integrating this, and using standard estimates (see [3]) we obtain:

$$|||(\vec{E}-\vec{\delta})(t)|||_E^2+|||(\vec{H}+\vec{\beta})(t)|||_H^2$$
$$\leq 2|||(\vec{E}-\vec{\delta})(0)|||_E^2+2|||(\vec{H}+\vec{\beta})(0)|||_H^2$$
$$+4\left(\int_0^t\left(|||\vec{\gamma}-\frac{d}{dt}\vec{\delta}|||_E+|||\vec{\alpha}+\frac{d}{dt}\vec{\beta}|||_H\right)ds\right)^2.$$

Now taking square roots of both sides, and using the fact that

$$|||\vec{E}(t)|||_E \leq |||\left(\vec{E}-\vec{\delta}\right)(t)|||_E+|||\vec{\delta}(t)|||_E$$

and

$$|||\vec{H}(t)|||_H \leq |||\left(\vec{H}+\vec{\beta}\right)(t)|||_H+|||\vec{\beta}(t)|||_H$$

together with the fact that $\vec{E}(0)=0$ and $\vec{H}(0)=0$ completes the proof. □

In [2] we showed how a simpler version of the above stability result, and a careful decomposition of the local truncation error, can be used to prove convergence of the FDTD scheme on arbitrary tensor product grids (including the grid shown in Figure 1). Precisely, we prove that

$$|||\vec{E}_e-\vec{E}\,|||_E+|||\vec{H}_e-\vec{H}\,|||_H=O(h^2+th^2),$$

where $\vec{E}_e$ (resp. $\vec{H}_e$) is the vector of exact values of $\boldsymbol{E}$ (resp. H) at the finite difference points and $\vec{E}$ and $\vec{H}$ are the semi-discrete Yee finite difference approximations described in this section. Thus, despite the uncentered difference for $E^{(2)}_{0,j}$, the method retains its second order convergence rate.

Of course there will be a spurious reflection from the interface at $x=0$ since a plane wave incident from $x<0$ will experience a change of grid at $x=0$. To quantify this reflection, we can analyze the reflection of a single frequency plane wave at the interface. We now suppose that the grid covers the entire plane (so that $L=\infty$), that $\boldsymbol{J}=0$, and that the discrete electromagnetic field is time harmonic so that

$$E^{(\gamma)}_{\alpha,\beta}=\hat{E}^{(\gamma)}_{\alpha,\beta}e^{-i\omega t}\text{ and }H_{\alpha,\beta}=\hat{H}^{(\gamma)}_{\alpha,\beta}e^{-i\omega t}\qquad(7)$$

for all valid choices of α,β and γ where ω is a constant. Using this assumption in the FDTD equations amounts to replacing $d/(dt)$ by $-i\omega$ and using "hat" variables. It will be convenient to work only with the scalar magnetic field for the reflection analysis so we eliminate the electric field variables and arrive at the following equations:

$$-\omega^2\hat{H}_{p,q} = \frac{1}{4h^2}\left(\hat{H}_{p+2,q}-2\hat{H}_{p,q}+\hat{H}_{p-2,q}\right)+\frac{1}{4h^2}\left(\hat{H}_{p,q+2}-2\hat{H}_{p,q}+\hat{H}_{p,q-2}\right)\qquad(8)$$

for $p=-(2l+1)$, $0<l<N$ and $q=2m+1$, $-N\leq m<N$;

$$-\omega^2\hat{H}_{p,q} = \frac{1}{h^2}\left(\hat{H}_{p+1,q}-2\hat{H}_{p,q}+\hat{H}_{p-1,q}\right)+\frac{1}{4h^2}\left(\hat{H}_{p,q+2}-2\hat{H}_{p,q}+\hat{H}_{p,q-2}\right),\qquad(9)$$

for $p=l+1/2$, $1\leq l\leq N-1$ and $q=2m+1$, $-N\leq m<N$;

$$-\omega^2\hat{H}_{-1,q}=\frac{1}{4h^2}\left(H_{-1,q+2}-2H_{-1,q}+H_{-1,q-2}\right)+\frac{1}{4h^2}\left(\frac{4}{3}H_{1/2,q}-\frac{7}{3}H_{-1,q}+H_{-3,q}\right)\qquad(10)$$

for $q=2m+1$, $-N\leq m<N$ and finally

$$-\omega^2H_{1/2,q}=\frac{1}{4h^2}\left(H_{1/2,q+2}-2H_{1/2,q}+H_{1/2,q-2}\right)+\frac{1}{h^2}\left(H_{3/2,q}-\frac{5}{3}H_{1/2,q}+\frac{2}{3}H_{-1,q}\right)\qquad(11)$$

for $q=2m+1$, $-N\leq m<N$. To perform the reflection analysis we assume that the discrete magnetic field in $x<0$ consists of an incident plane wave and a reflected plane wave with amplitude R so that

$$\hat{H}_{\alpha,\beta} = \exp(i(k_1x_\alpha+k_2y_\beta))+R\exp(i(-k_1x_\alpha+k_2y_\beta))\qquad(12)$$

for all valid α and β if $\alpha<0$. In $x>0$ the discrete magnetic field consists of a plane wave transmitted through the artificial grid interface at $x=0$. Thus if $\alpha>0$

$$\hat{H}_{\alpha,\beta}=T\exp(i(k_1'x_\alpha+k_2y_\beta))\qquad(13)$$

here k_1, k_2 and k_1' are the wave numbers which are unknown. The amplitudes T and R must also be found. Obviously, if the method handled the mesh interface at $x=0$ transparently, we would have $T=1, R=0$ and $k_1'=k_1$. Due to the mesh interface this will not be exactly true.

Substituting (12) in (8) we conclude that (8) is satisfied provided the standard semi-discrete Yee dispersion relation holds. This implies that k_1 and k_2 must be chosen so that

$$\omega^2h^2=\sin^2(k_1h)+\sin^2(k_2h).\qquad(14)$$

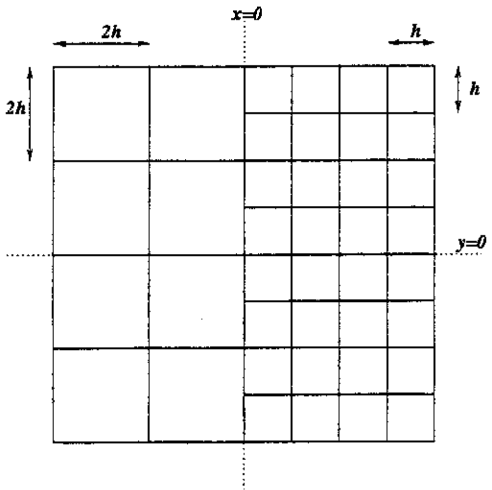

Figure 3: A typical grid for the sub-gridded Yee scheme analyzed in this paper.

Similarly, if (13) is substituted into (9) we can see that (9) is satisfied provided k_1' is chosen so that

$$\omega^2 h^2 = 4\sin^2\left(\frac{k_1' h}{2}\right) + \sin^2(k_2 h). \qquad (15)$$

For given ω and k_2, it is obvious that $k_1' \neq k_1$ and so a spurious reflection occurs at $x = 0$. Next we substitute (12) and (13) into (10) and (11) (using the assumption that (14) and (15) hold). Thanks to MAPLE we can then obtain a series expansion for R and T in terms of h as follows

$$R = \frac{3}{16}(\omega^2 - k_2^2)h^2 + O(h^4), \qquad (16a)$$

$$T = 1 - \frac{3}{16}\left(\omega^2 - k_2^2\right) + O(h^4). \qquad (16b)$$

It is a little surprising that the reflection and transmission error is $O(h^2)$, since we know that even if the grid changes by arbitrary stretchings in the x and y directions, the overall error is $O(h^2)$.

The above results give a reference by which to compare the results in the remainder of the paper. We would like to develop a sub-gridding extension of the FDTD scheme keeping an $O(h^2)$ global error and keeping the reflection and transmission error of order similar to that in (16a)–(16b). Of course it might be useful to improve on the reference. For example it might be possible to improve the reflection at the interface by a move complicated interpolation strategy. We will not pursue that direction here.

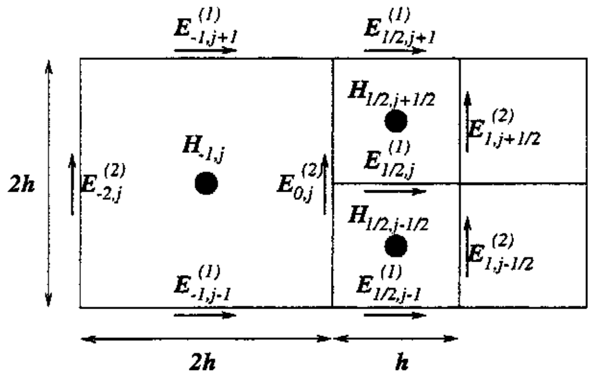

Figure 4: A diagram of the cells either side of $x = 0$. At $x = 0$ the grid size is decreased by a factor of 2.

4 A Simple Method

In this section we shall present and analyze a simple sub-gridding technique. The method is based on piecewise constant interpolation. Note that if we want to use the stability estimate in Theorem 1, we are not free to choose arbitrary interpolation for the electric and magnetic field values since the final equations must have the form of (5a) and (5b).

We now assume that the mesh in $x > 0$ is refined by a factor 1/2 in the x and y directions compared to the mesh for $x < 0$. Figure 3 shows such a mesh. All elements in the mesh are squares, but the grid is refined abruptly at $x = 0$. In the regions $x > 0$ and $x < 0$, the standard Yee unknowns will be used (i.e., on the edges and centroids of the mesh). Along $x = 0$, we use the degrees of freedom associated with the coarser mesh. Figure 4 shows cells either side of $x = 0$ and indicates the location of the finite difference values.

Now we can write down the sub-gridded FDTD equations. The equations for all the unknowns in $x < 0$ are the same as in the previous section. See for example (4a) - (4c). Similarly, all unknowns in $x \geq h$ satisfy standard FDTD equations, as does $E^{(1)}_{1/2,j}$ for $-2N+1 \leq j \leq 2N-1$. The only changes are in the equations for $E^{(2)}_{0,j}$, $H_{1/2,j+1/2}$ and $H_{1/2,j-1/2}$, $j = 2l+1$, $-N \leq l < N$. We start with the magnetic field. If we use the standard Yee scheme for $H_{1/2,j+1/2}$ we would need a value for $E^{(2)}_{0,j+1/2}$. Extending $E^{(2)}_{0,j}$ by a constant we use $E^{(2)}_{0,j+1/2} = E^{(2)}_{0,j}$ (this amounts to using a one-sided integration rule in the contour path extension of the Yee scheme). Similarly $E^{(2)}_{0,j-1/2} = E^{(2)}_{0,j}$. Thus the equations for $H_{1/2,j+1/2}$ and $H_{1/2,j-1/2}$ are (for $j = 2l+1$,

$-N \le l < N$)

$$h^2 \frac{d}{dt} H_{1/2,j+1/2} - h\left(E^{(1)}_{1/2,j+1} - E^{(1)}_{1/2,j}\right) + h\left(E^{(2)}_{1,j+1/2} - E^{(2)}_{0,j}\right) = 0, \tag{17}$$

$$h^2 \frac{d}{dt} H_{1/2,j-1/2} - h\left(E^{(1)}_{1/2,j} - E^{(1)}_{1/2,j-1}\right) + h\left(E^{(2)}_{1,j-1/2} - E^{(2)}_{0,j}\right) = 0. \tag{18}$$

Now that we have a complete set of equations for the magnetic field variables, we know that the vectors of unknown $\vec{E}$ and $\vec{H}$ satisfy (5b) with a suitable choice of M_H and C^T. Thus the equations for $\vec{E}$ can be obtained from (5a) (i.e., we are not free to choose the interpolation scheme for both equations at the same time). Then since Theorem 3.1 is satisfied the method will be stable. The following equation for $E^{(2)}_{0,j}$ results:

$$3h^2 \frac{d}{dt} E^{(2)}_{0,j} - 2hH_{-1,j} + h\left(H_{1/2,j+1/2} + H_{1/2,j-1/2}\right) = -3h^2 J^{(2)}_{0,j}. \tag{19}$$

Notice the similarity between this equation and equation (4d). It is interesting to note that the piecewise constant interpolation used in writing down (17) and (18) gives rise to a piecewise linear interpolation of H in (19).

In order to analyze the convergence rate of the scheme outlined above, we can apply Theorem 3.1. Since we have a uniform mesh for $x < 0$ and $x > 0$, we know that apart from the equations for $E^{(2)}_{0,j}$, $H_{1/2,j+1/2}$ and $H_{1/2,j-1/2}$, the local truncation error is second order. Equation (17) has a constant local truncation error since $E^{(2)}_{0,j}$ is an $O(h)$ approximation to $E^{(2)}_{0,j+1/2}$. More precisely, if $\boldsymbol{E}(\boldsymbol{x},t)$ and $H(\boldsymbol{x},t)$ satisfy (1a) and (1b)

$$\begin{aligned} & h^2 \frac{\partial}{\partial t} H(x_{1/2}, y_{j+1/2}, t) \\ & \quad - h\left(E^{(1)}(x_{1/2}, y_{j+1}, t) - E^{(1)}(x_{1/2}, y_j, t)\right) \\ & \quad + h\left(E^{(2)}(x_1, y_{j+1/2}, t) - E^{(2)}(x_0, y_j, t)\right) \\ = \; & \frac{h^2}{2}\frac{\partial E^{(2)}}{\partial y}(x_0, y_j, t) + O\left(h^3\right), \end{aligned}$$

and

$$\begin{aligned} & h^2 \frac{\partial}{\partial t} H\left(x_{1/2}, y_{j-1/2}, t\right) \\ & \quad - h\left(E^{(1)}\left(x_{1/2}, y_j, t\right) - E^{(1)}\left(x_{1/2}, y_{j-1}, t\right)\right) \\ & \quad + h\left(E^{(2)}\left(x_1, y_{j-1/2}, t\right) - E^{(2)}\left(x_0, y_j, t\right)\right) \\ = \; & -\frac{h^2}{2}\frac{\partial E^{(2)}}{\partial y}\left(x_0, y_j, t\right) + O\left(h^3\right). \end{aligned}$$

Thus we define the mesh function $\vec{\delta}$, defined on edges in the grid, by $\delta^{(2)}_{\alpha,\beta} = 0$ for all valid choices of α and β corresponding to vertical edges in the mesh and

$$\delta^{(1)}_{\alpha,\beta} = \frac{h}{2}\frac{\partial E^{(2)}}{\partial y}(x_0, y_j, t) \tag{20}$$

if $\alpha = 1/2$, $\beta = j$, where $j = 2l+1$, $-N \le l < N$ and $\delta^{(1)}_{\alpha,\beta} = 0$ otherwise. Then we have that if $\vec{e}^E = \vec{E}_e - \vec{E}$ and $\vec{e}^H = \vec{H}_e - \vec{H}$,

$$M_H \frac{\partial \vec{e}^H}{\partial t} + C^T \vec{e}^E = C^T \vec{\delta} + M_H \vec{\alpha} \tag{21}$$

and furthermore $\vec{\alpha} = \vec{\alpha}_1 h + O(h^2)$ where $\vec{\alpha}_1$ is non-zero only for those unknowns associated with the strip $0 \le x \le h$. The point of this estimate is that the local truncation error has been decomposed into the discrete curl of a first order quantity plus first order quantities.

It remains to analyze the local truncation error in the electric field equations. Except for the equation for $E^{(2)}_{0,j}$ (see (19)) all the remaining electric field equations are centered FDTD equations so the local truncation error for these equations is second order. For (19) we know that

$$H_{1/2,j+1/2} + H_{1/2,j-1/2} = 2H_{1/2,j} + O(h^2).$$

Hence the local truncation error in (19) is first order. Putting the electric field equations together in matrix form, we see that

$$M_E \frac{\partial \vec{e}^E}{\partial E} - C\vec{e}^H = M_E \vec{\gamma} \tag{22}$$

where $\vec{\gamma} = \vec{\gamma}_1 h + O(h^2)$. $\vec{\gamma}_1$ is non-zero only for degrees of freedom lying on $x = 0$ (i.e., from (19)).

We have not to attempted to decompose the electric field error further since the simple analysis used to obtain (22) gives a similar form to that obtained for the magnetic field equations in (21).

Applying Theorem 3.1, we conclude that

$$|||\vec{e}^E|||_E + |||\vec{e}^H|||_H \le C\left(\max_{0\le s\le t} |||\vec{\delta}\,|||_E + \int_0^t \left(|||\alpha|||_H |||\vec{\gamma}|||_E + |||\frac{d\vec{\delta}}{dt}|||_E\right) ds\right)$$

But $|||\vec{\delta}|||_E = \sqrt{\vec{\delta}^{\,T} M_E \vec{\delta}} = O\left(h^{3/2}\right)$ since $\vec{\delta}$ is given by (20) so that only $O(1/h)$ entries are non-zero. By (20) each non-zero entry is $O(h)$ and M_E is diagonal with entries $O(h^2)$ so $\sqrt{\vec{\delta}^{\,T} M_E \vec{\delta}} = \sqrt{O(h^2)O(1/h)O(h)O(h)}$. Similarly since $\vec{\alpha} = \vec{\alpha}_1 h + O(h^2)$ with $\vec{\alpha}_1$ non-zero only for those degrees of freedom within $O(h)$ of $x = 0$, we have $|||\vec{\alpha}|||_H = O(h^{3/2})$, and similarly $|||\vec{\gamma}|||_H = O(h^{3/2})$. We have thus proved the following theorem:

Theorem 4.1 *Suppose $\vec{E}$ and $\vec{H}$ are computed using the semi-discrete simple method, and $\vec{E}_e$ and $\vec{H}_e$ are the corresponding vectors of exact solution values, then*

$$|||\vec{E}-\vec{E}_e|||_E + |||\vec{H}-\vec{H}_e|||_H = O(h^{3/2}+th^{3/2}).$$

Remark. This estimate is not as good as the estimate for the unsub-gridded case given in the previous section, but the estimate may well be pessimistic as we shall show by a computational example and by a reflection analysis.

Next let us perform a reflection analysis at the interface $x=0$. This is slightly more complex than the analysis of the standard FDTD at a grid interface (see the previous section). Again we move to the frequency domain using (7). Then we eliminate the electric field to obtain a system of equations involving only the magnetic field equations.

For magnetic field variables in $x<-2h$, the standard FDTD discretization yields, as before (8). For $\hat{H}_{-1,j}$, $j=2l+1$, $-\infty<l<\infty$, we obtain

$$\begin{aligned}-\omega^2\hat{H}_{-1,j} &= \frac{1}{4h^2}\left(\hat{H}_{-1,j+1}-2\hat{H}_{-1,j}+\hat{H}_{-1,j-1}\right)\\ &+\frac{1}{4h^2}\left(\frac{2}{3}\left(\hat{H}_{1/2,j+1/2}+\hat{H}_{1/2,j-1/2}\right)\right.\\ &\left.-\frac{7}{3}\hat{H}_{-i,j}+\hat{H}_{-3,j}\right)\end{aligned}$$

For magnetic field variables in $0<x<h$ we obtain:

$$\begin{aligned}&-\omega^2\hat{H}_{1/2,j+1/2}\\ &= \frac{1}{h^2}\left(\hat{H}_{1/2,j+3/2}-2\hat{H}_{1/2,j+1/2}+\hat{H}_{1/2,j-1/2}\right)\\ &+\frac{1}{h^2}\left(\hat{H}_{3/2,j+1/2}-\frac{4}{3}\hat{H}_{1/2j+1/2}\right.\\ &\left.-\frac{1}{3}\hat{H}_{1/2,j-1/2}+\frac{2}{3}\hat{H}_{-1,j}\right), \qquad (23)\end{aligned}$$

$$\begin{aligned}&-\omega^2\hat{H}_{1/2,j-1/2}\\ &= \frac{1}{h^2}\left(\hat{H}_{1/2,j+1/2}-2\hat{H}_{1/2,j-1/2}+\hat{H}_{1/2,j-3/2}\right)\\ &+\frac{1}{h^2}\left(\hat{H}_{3/2,j-1/2}-\frac{1}{3}\hat{H}_{1/2,j+1/2}\right.\\ &\left.-\frac{4}{3}\hat{H}_{1/2,j-1/2}+\frac{2}{3}\hat{H}_{-1,j}\right), \qquad (24)\end{aligned}$$

(25)

for $j=2l+1$, $-\infty\le l\le\infty$. For $x>h$, the standard Yee scheme on the sub-grid yields

$$\begin{aligned}\omega^2\hat{H}_{p,q} &= \frac{1}{h^2}\left(\hat{H}_{p+1,q}-2\hat{H}_{p,q}+\hat{H}_{p-1,q}\right) \qquad (26)\\ &+\frac{1}{h^2}\left(\hat{H}_{p,q+1}-2\hat{H}_{p,q}+\hat{H}_{p,q-1}\right)\end{aligned}$$

for $p=r+1/2$, $0<r<\infty$ and $q=s+1/2$, $-\infty<r<\infty$. From the above equations (or Figure 4) we can see that the stencil repeats on a period of $2h$ in the y direction (i.e. if we move a distance $2h$ upward or downwards in the grid then the same equation holds). Thus we assume that for all valid choices of α and β

$$\hat{H}_{\alpha,\beta+2}=\hat{H}_{\alpha,\beta}e^{2ik_2h}. \qquad (27)$$

Using this in (8), (23), (23), (24) and (26) results in a set of five equations defined on the strip $-\infty\le x\le\infty$ and $0\le y<2h$. Now we assume that for $x<2h$ the magnetic field is made up of a reflected and incident part, so for $l\ge 0$, $j=-(2l+1)$, we have:

$$H_{j,0}=e^{ihk_1j}+Re^{-ihk_1j}. \qquad (28)$$

Using this and (27) and (28) in (8) shows that (8) is satisfied provided k_1 and k_2 satisfy (14). For $x>h$, we want to choose $\hat{H}$ to be a discrete plane wave. If we choose

$$\begin{aligned}\hat{H}_{l+1/2,1/2} &= \alpha e^{i(l+1/2)k_1'h}e^{ihk_2/2}, \qquad (29a)\\ \hat{H}_{l+1/2,-1/2} &= \beta e^{i(l+1/2)k_1'h}e^{-ihk_2/2}, \qquad (29b)\end{aligned}$$

and use these definitions in (26) for $p=l+\frac{1}{2}$, $q=\frac{1}{2}$ and $p=l+\frac{1}{2}$, $q=-\frac{1}{2}$, $l>0$ we find that the following equations must be satisfied by k_1', α and β:

$$\begin{aligned}-\omega^2h^2\alpha &= 2\cos(k_2h)\beta-2\alpha-4\sin^2\left(\frac{k_1'h}{2}\right)\alpha,\\ -\omega^2h^2\beta &= 2\cos(k_2h)\alpha-2\beta-4\sin^2\left(\frac{k_1'h}{2}\right)\beta.\end{aligned}$$

This is a homogeneous matrix equation for α and β and so, to have a non-trivial solution, the determinant must vanish. Thus

$$\left(\omega^2h^2-2-4\sin^2\left(\frac{k_1'h}{2}-\right)\right)^2=4\cos^2(k_2h),$$

and thus we have two values for k_1'. The first is the "physical" value of k_1' which satisfies

$$\omega^2h^2-2+4\sin^2\left(\frac{k_1'h}{2}\right)=-2\cos(k_2h).$$

After a little manipulation this is exactly (15). We denote this root $k_1^{(1)}$. Using MAPLE we find that

$$k_1^{(1)}=\sqrt{\omega^2-k_2^2}+O(h^2)$$

which justifies the "physical" label. The other root, which we denote $k_1^{(2)}$ satisfies

$$\omega^2h^2-2+4\sin^2\left(\frac{k_1^{(2)}h}{2}\right)=2\cos(k_2h). \qquad (30)$$

In this case MAPLE gives

$$k_2^{(2)} = \frac{\pi}{h} - \sqrt{\omega^2 + k_2^2} + O(h^2).$$

This is a spurious mode.

Corresponding to $k_1' = k_1^{(1)}$ in, we have the eigenvector

$$\begin{pmatrix} \alpha \\ \beta \end{pmatrix} = \begin{pmatrix} 1 \\ 1 \end{pmatrix}$$

and corresponding to $k_1' = k_1^{(2)}$ we have

$$\begin{pmatrix} \alpha \\ \beta \end{pmatrix} = \begin{pmatrix} 1 \\ -1 \end{pmatrix}.$$

Thus we must allow for two transmitted waves at the interface with amplitude factors T_1 and T_2. So we assume that for $l > 0$

$$H_{l+1/2,1/2} = \left(T_1 e^{i(l+1/2)k_1^{(1)}h} + T_2 e^{i(l+1/2)k_1^{(2)}h}\right) e^{ihk_2/2}, \tag{31a}$$

$$H_{l+1/2,-1/2} = \left(T_1 e^{i(l+1/2)k_1^{(1)}h} - T_2 e^{i(l+1/2)k_1^{(2)}h}\right) e^{-ihk_2/2}. \tag{31b}$$

There are three unknowns, T_1 and T_2 from above and R from (28). We substitute for H in (23), (23) and (24), giving a system of three linear equations for T_1, T_2 and R. Using MAPLE these can be solved to yield

$$R = \frac{3\omega^4 - 8\omega^2 k_2^2 + 6k_2^4}{16(\omega^2 - k_2^2)} h^2 + O(h^3), \tag{32a}$$

$$T_1 = 1 - \frac{3\omega^4 + 2k_2^4 - 6\omega^2 k_2^2}{16(\omega^2 - k_2^2)} h^2 + O(h^3), \tag{32b}$$

$$T_2 = \frac{i}{12}\sqrt{\omega^2 - k_2^2}\, k_2 h^2 + O(h^3), \tag{32c}$$

provided $k_2 \neq \omega$.

Thus the order of accuracy of the reflection and transmission coefficients of the simple sub-gridded method described in this section are the same as for the FDTD scheme at an interface between grids of different sizes (see (16a)–(16b)). The difference is that the simple sub-gridding scheme has a spurious mode with amplitude proportional to h^2. These results suggest (and this is what we observe computationally) that the simple method will be second order accurate rather than 3/2 order as our error analysis predicts.

5 A Linear Interpolation Method

Other authors have suggested using higher order interpolation to construct sub-gridded schemes. Here we analyze a scheme based on linear interpolation similar to a semi-discrete version of the scheme in [5]. The model problem in Figure 3 is not suitable for this method since it is difficult to handle the interface if it hits a boundary. This is unlikely to be a problem in practice, but to avoid it here we shall only perform a reflection analysis assuming an infinite interface. The arrangement of unknowns is the same as for the simple scheme in the previous section (see Figure 4).

We start by writing down the equations for $H_{1/2,j+1/2}$ and $H_{1/2,j-1/2}$, $j = 2l+1$, $-\infty < l < \infty$. To write down the equation for $H_{1/2,j+1/2}$ we need $E^{(2)}_{0,j+1/2}$ and we obtain this by linear interpolation between the closest values of $E^{(2)}$ in the grid (rather than by constant interpolation as used in the previous section) thus

$$E^{(2)}_{0,j+1/2} = \frac{3}{4}E^{(2)}_{0,j} + \frac{1}{4}E^{(2)}_{0,j+2}$$

and hence

$$h^2\frac{d}{dt}H_{1/2,j+1/2} - h\left(E^{(1)}_{1/2,j+1} - E^{(1)}_{1/2,j}\right) + h\left(E^{(2)}_{1,j+1/2} - \frac{3}{4}E^{(2)}_{0,j} - \frac{1}{4}E^{(2)}_{0,j+2}\right) = 0. \tag{33}$$

Similarly for $H_{1/2,j-1/2}$ we obtain:

$$h^2\frac{d}{dt}H_{1/2,j-1/2} - h\left(E^{(1)}_{1/2,j} - E^{(1)}_{1/2,j-1}\right) + h\left(E^{(2)}_{1,j-1/2} - \frac{3}{4}E^{(2)}_{0,j} - \frac{1}{4}E^{(2)}_{0,j-2}\right) = 0. \tag{34}$$

The remaining magnetic field equations are standard FDTD equations. Now that we have specified the magnetic field equations, the electric field equations are determined so as to have the form of (5a)–(5b). This implies that standard FDTD equations hold for all electric field variables except those on $x = 0$. On $x = 0$ the following equation holds:

$$3h^2\frac{d}{dt}E^{(2)}_{0,j} - \left(2hH_{-i,j} - \frac{3}{4}hH_{1/2,j+1/2} - \frac{3}{4}hH_{1/2,j-1/2} - \frac{1}{4}hH_{1/2,j+3/2} - \frac{1}{4}hH_{1/2,j-3/2}\right) = -3h^2 J_{0,j}, \tag{35}$$

for $j = 2l+1$, $-\infty < l < \infty$.

The reflection analysis can be performed in exactly the same way as for the simple scheme analyzed in the previous section. We start by assuming a time harmonic profile using (7). Then we eliminate the electric field and obtain equations for the magnetic field alone. For the magnetic field variables in $x < -2h$, the standard FDTD discretization (8) holds, and for $x > h$ (26) holds as before.

The equation for $\hat{H}_{-1,j}$, $j = 2l+1$, $-\infty < l < \infty$ is

$$-\omega^2\hat{H}_{-1,j} = \frac{1}{4h^3}\left(\hat{H}_{-1,j+2} - 2\hat{H}_{-1,j} + \hat{H}_{-1,j-2}\right) \quad (36)$$
$$+\frac{1}{4h^2}\left(\hat{H}_{-3,j} - \frac{7}{3}\hat{H}_{-1,j} + \frac{1}{2}\left(\hat{H}_{1/2,j+1/2}+\right.\right.$$
$$\left.\left.H_{1/2,j-1/2}\right) + \frac{1}{6}\left(\hat{H}_{1/2,j+3/2} + \hat{H}_{1/2,j-3/2}\right)\right).$$

For $\hat{H}_{1/2,j+1/2}$ and $\hat{H}_{1/2,j-1/2}$ we obtain

$$\begin{aligned}-\omega^2\hat{H}_{1/2,j+1/2} = &\\ &\frac{1}{h^2}\left(\hat{H}_{1/2,j+3/2} - 2\hat{H}_{1/2,j+1/2} + \hat{H}_{1/2,j-1/2}\right)\\ &+\frac{1}{h^2}\left(\hat{H}_{3/2,j+1/2} - \hat{H}_{1/2,j+1/2}\right) \qquad (37)\\ &+\frac{3}{4h^2}\left(\frac{2}{3}\hat{H}_{-1,j} - \frac{1}{4}\left(\hat{H}_{1/2,j+1/2} + \hat{H}_{1/2,j-1/2}\right)\right.\\ &\left.-\frac{1}{12}\left(\hat{H}_{1/2,j+3/2} + \hat{H}_{1/2,j-3/2}\right)\right)\\ &+\frac{1}{4h^2}\left(\frac{2}{3}\hat{H}_{-1,j+2} - \frac{1}{4}\left(\hat{H}_{1/2,j+5/2} + \hat{H}_{1/2,j+3/2}\right)\right.\\ &\left.-\frac{1}{12}\left(\hat{H}_{1/2,j+7/2} + \hat{H}_{1/2,j+1/2}\right)\right),\end{aligned}$$

and

$$\begin{aligned}-\omega^2 H_{1/2,j-1/2} = &\\ &\frac{1}{h^2}\left(H_{1/2,j+1/2} - 2H_{1/2,j-1/2} + H_{1/2,j-3/2}\right)\\ &+\frac{1}{h^2}\left(H_{3/2,j-1/2} - H_{1/2,j-1/2}\right) \qquad (38)\\ &+\frac{3}{4h^2}\left(\frac{2}{3}H_{-1,j} - \frac{1}{4}\left(H_{1/2,j+1/2} + H_{1/2,j-1/2}\right)\right.\\ &\left.-\frac{1}{12}\left(H_{1/2,j+3/2} + H_{1/2,j-3/2}\right)\right)\\ &+\frac{1}{4h^2}\left(\frac{2}{3}H_{-1,j-2} - \frac{1}{4}\left(H_{1/2,j-3/2} + H_{1/2,j-5/2}\right)\right.\\ &\left.-\frac{1}{12}\left(H_{1/2,j-1/2} + H_{1/2,j-7/2}\right)\right).\end{aligned}$$

As before, we assume that in $x \le 0$

$$\hat{H}_{\alpha,\beta} = \left(e^{ik_1 2\alpha h} + Re^{-ik_1 2\alpha h}\right)e^{ik_2 2\beta h} \qquad (39)$$

and require that k_1 satisfy (14) so that (8) is satisfied. For $x > 0$ we use $\hat{H}_{\alpha,\beta}$ given by (31a)–(31b) and require that $k_1^{(1)}$ satisfy (15) and $k_1^{(2)}$ satisfy (30). Then (26) is satisfied. Using (39) and (31a)–(31b) in (36), (37) and (38) yields a linear system for $R, T^{(1)}$ and $T^{(2)}$. Via MAPLE we obtain (provided $k_2 \neq \omega$)

$$R = \frac{1}{16}\left(\frac{3\omega^4 - 12\omega^2k_2^2 + 10k_2^4}{\omega^2 - k_2^2}\right)h^2 + O(h^3),$$

$$T^{(1)} = 1 - \frac{1}{16}\left(\frac{3\omega^4 - 6\omega^2k_2^2 + 2k_2^4}{\omega^2 - k_2^2}\right)h^2 + O(h^3),$$

$$T^{(2)} = \frac{i}{48}\sqrt{\omega^2 - k_2^2}k_2^3h^4 + O(h^5).$$

Compared to (32a)–(32c) we can see that R and $T^{(1)}$ are of the same order of accuracy for the linear interpolation case studied here and for the simple method in the previous section. The only obvious gain of using the linear method is that the spurious transmitted mode with amplitude $T^{(2)}$ is now greatly decreased compared to (32c) ($T^{(2)} = O(h^4)$ rather than $O(h^2)$ for the simple method).

6 Numerical Results

The error estimate for the simple sub-gridding scheme predicts an $O(h^{3/2})$ rate of convergence, whereas the reflection analysis suggests an $O(h^2)$ rate. In this section we present the results of a simple numerical experiment which shows that, at least in the case studied here, the method is second order convergent.

The problem we study is the propagation of a Gaussian wave across the square $[0,2]\times[0,2]$. The exact wave is given by

$$\boldsymbol{E}_e(\boldsymbol{x},t) = \begin{pmatrix} k_2 \\ -k_1 \end{pmatrix} g(t-\boldsymbol{k}\cdot\boldsymbol{x}), \quad H_e(\boldsymbol{x},t) = -g(t-\boldsymbol{k}\cdot\boldsymbol{x}),$$

where $\boldsymbol{k} = (\cos(1),\sin(1))^T$ and $g(s) = \exp(-10(s-1)^2)$. The boundary conditions are chosen to introduce the wave into the square (and $\boldsymbol{J} = 0$). We use a mesh like that in Figure 3 with a sudden change in the mesh size at $x = 0$ and, as before, define the mesh parameter h to be the size of the mesh squares in the finer mesh. We use leapfrog time stepping with a uniform time-step of $\Delta t = h/\sqrt{2}$ (which is not optimal for the coarser grid—see [5] for suggestions about an improved strategy).

Figure 5 shows a log-log plot of the discrete error in the magnetic field defined by $|||\vec{H}_e - \vec{H}|||_H$ against h together with a reference line for $O(h^2)$ convergence. It is clear that the method is showing second order convergence.

7 Conclusion

We have provided some preliminary analysis of two sub-gridding schemes. In order to guarantee stability, we have constructed the schemes by applying interpolation only to evaluate the electric field at the interface. Symmetry considerations then force the magnetic field to be

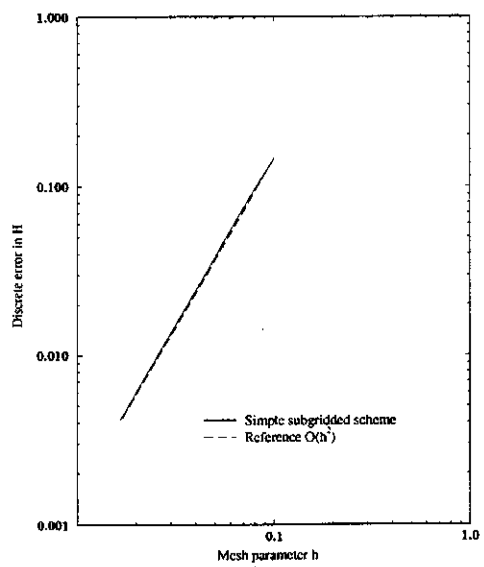

Figure 5: A log-log plot of the error $|||\vec{H}_e - \vec{H}|||_H$ against the mesh parameter h and a reference line showing $O(h^2)$ convergence. Clearly, for this example, the simple sub-gridding scheme is exhibiting $O(h^2)$ convergence rather than $O(h^{3/2})$ as predicted by theory.

interpolated in a way to guarantee stability (this reduces flexibility in constructing the sub-gridding scheme).

Our analysis shows that the simple scheme employing constant interpolation performs surprisingly well. It is provably $O(h^{3/2})$ convergent, and simple numerical experiment together with a reflection analysis suggest that the method can be $O(h^2)$ accurate in practice.

The linear interpolation scheme analyzed in section 5 has the advantage of improving the amplitude of the transmitted spurious mode, but the reflected mode is still only second order. The use of this method when the grid interface intersects a boundary presents a problem.

Clearly, the real problem is three dimensional, so the analysis started in this paper needs to be extended to three dimensions. In addition the application of the linear scheme at boundaries needs to be investigated.

References

[1] K. Yee, "Numerical solution of initial boundary value problems involving Maxwell's equations in isotropic media," *IEEE Trans. on Antennas and Propagation*, vol. AP–16, pp. 302–307, 1966.

[2] P. Monk and E. Süli, "Error estimates for Yee's method on non-unfirm grids," *IEEE Trans. on Magnetics*, vol. 30, pp. 3200–3203, 1994.

[3] P. Monk and E. Süli, "A convergence analysis of Yee's scheme on non-uniform grids," *SIAM J. on Numer. Anal.*, vol. 31, pp. 393–412, 1994.

[4] K. Kunz and L. Simpson, "A technique for increasing the resolution of finite-difference solutions of the Maxwell equations," *IEEE Transactions on Electromagnetic Compatibility*, vol. EMC-23, pp. 419–422, 1981.

[5] I. Kim and W. Hoefer, "A local mesh refinement algorithm for the time domain-finite difference method using Maxwell's curl equations," *IEEE Transactions on Microwave Theory and Techniques*, vol. 38, pp. 812–185, 1990.

[6] S. Zivanovic, K. Yee, and K. Mei, "A subgridding method for the time-domain finite difference method to solve Maxwell's equations," *IEEE Transactions on Microwave Theory and Techniques*, vol. 39, pp. 471–479, 1991.

[7] D. Prescott and N. Shuley, "A method for incorporating different sized cells into the finite-difference time-domain analysis technique," *IEEE Microwave and Guided Wave Letters*, vol. 2, pp. 434–436, 1992.

[8] R. Ewing, R. Lazarov, and P. Vassilevski, "Local refinement techniques for elliptic problems on cell-centered grids: I. Error analysis," *Mathematics of Computation*, vol. 56, pp. 437–461, 1991.

[9] R. Ewing et al., "Some grid refinement schemes for hyperbolic equations with piecewise constant coefficients," *Math. Comp.*, vol. 56, pp. 61–86, 1991.

[10] M. Berger and J. Oliger, "Adaptive mesh refinement for hyperbolic partial differential equations," *J. Comp. Phys.*, vol. 53, pp. 484–512, 1984.

[11] T. Weiland, "Numerical solution of Maxwell's equation for static, resonant and transient problems," in *Studies in Electrical and Electronic Engineering 28B* (T. Berceli, ed.), (New York), pp. 537–542, URSI International Symposium on Electromagnetic Theory Part B, Elsevier, 1986.